High-Speed, Low-Driving-Voltage Dual-Drive InP-Based Mach-Zehnder Modulator

Nobuhiro KIKUCHI[†a], ***Member*, Ken TSUZUKI**[†], ***Nonmember*, Takeshi KUROSAKI**[†],
Yasuo SHIBATA[†], ***and* Hiroshi YASAKA**[††], ***Members***

SUMMARY   We present a dual traveling-wave electrode InP-based Mach-Zehnder (MZ) modulator with an *n-i-n* waveguide structure. An electrical input/output interface placed on one side of the chip helps us to drive the modulator in a push-pull configuration. This configuration provides the modulator with great advantages such as reduced driving voltage amplitude, chirp-free operation, and the ability to support advanced modulation formats. The fabricated modulator exhibits good performance. A 40 Gb/s non-return-to-zero (NRZ) signal is successfully generated with a low driving of 1.3 V_{pp}. In addition, a 10-Gb/s optical duobinary (DB) signal is successfully generated and transmitted over a 240-km single-mode fiber (SMF). We also developed a wavelength tunable transmitter hybrid integrated with a modulator with a wavelength tunable laser. Full *C*-band 10-Gb/s operation and a 100-km SMF transmission with a low power penalty are confirmed.
key words: *Mach-Zehnder modulator, n-i-n structure, InP*

1. Introduction

The ever-increasing volume of data traffic on the internet is driving the demand for high-speed, large-capacity optical communication networks. One of the key components of these networks is a high-speed optical modulator. A LiNbO$_3$ (LN) Mach-Zehnder (MZ) modulator is a promising candidate, and it has been deployed in commercial optical long-haul transmission systems. However, the drawback is that it generally needs a relatively large driving voltage. Moreover, it suffers from bias instability, and requires a large package. In contrast, a semiconductor-based MZ modulator is very attractive because of its small chip size and potential for monolithic integration with semiconductor active devices such as laser diodes [1]–[4]. We have recently developed a traveling-wave electrode InP-based MZ modulator, which has a novel *n-i-n* isotype heterostructure [5]. The advantage of this structure over the conventional *p-i-n* structure is that it can eliminate electrical and optical losses originating from a *p*-doped layer. This enables the modulator to operate at both a high bit rate and a low driving voltage. The *n-i-n* MZ modulator also shows very low wavelength dependence.

Today, advanced modulation formats such as optical duobinary (DB) [6] and return-to-zero differential (quadra-

ture) phase-shift keying (RZ-D(Q)PSK) [7]–[9] have received increased attention in relation to systems operating at more than 40 Gb/s because they offer high spectral efficiency and robustness against fiber dispersion. These signals should be chirp-free. Moreover, even for conventional on-off keying (OOK), chirp control is very important in terms of increasing the transmission distance. For instance, with a 10-Gb/s NRZ format, a chirp-free or a negative chirp signal is needed to achieve an SMF transmission of more than 80 km. Against the above background, there is a strong need for a dual-electrode MZ modulator driven in a push-pull configuration. The push-pull configuration also offers another benefit, namely the driving voltage amplitude can be reduced to half that needed for a single-end configuration.

In this paper, we present a dual-drive, high-speed InP-based MZ modulator. For ease of connection with differential output driver integrated circuits (ICs), the electrical input/output interface of the dual electrode is placed on one side of the chip. In Sect. 2, we describe the design of our dual-drive traveling-wave electrode MZ modulator. We used the developed modulator chip to realize a compact MZ modulator module, and we demonstrate its performance as regards 40-Gb/s NRZ signal generation and 10-Gb/s optical DB signal generation in Sect. 3. Finally, as an additional application of our modulator, we also discuss a compact wavelength tunable transmitter module, which contains a tunable laser diode and our MZ modulator, and we report its performance with a 10-Gb/s NRZ signal in Sect. 4.

2. Design of Dual Traveling-Wave Electrode InP MZ Modulator

Figure 1(a) shows a schematic diagram of our new InP-based dual traveling-wave electrode Mach-Zehnder modulator chip that we designed to be driven in a push-pull configuration. In the electro-optic (E/O) interaction section, a grounded coplanar waveguide is formed on a high-mesa optical waveguide structure buried in benzocyclobutene (BCB) as shown in Fig. 1(b). The semiconductor layer stack consists of an *n*-doped lower cladding layer, an undoped core layer, an Fe-doped semi-insulating (SI) InP cladding layer, and an *n*-doped upper cladding layer, which are grown on an *SI*-InP substrate. This gives the waveguide an *n-i-n* isotype heterostructure [5]. The core layer is composed of a 0.2-μm-thick InGaAlAs/InAlAs multiple quantum well (MQW) layer ($\lambda_{PL} = 1.37\,\mu$m) with 0.05-μm-thick InGaAsP (1.3-μm
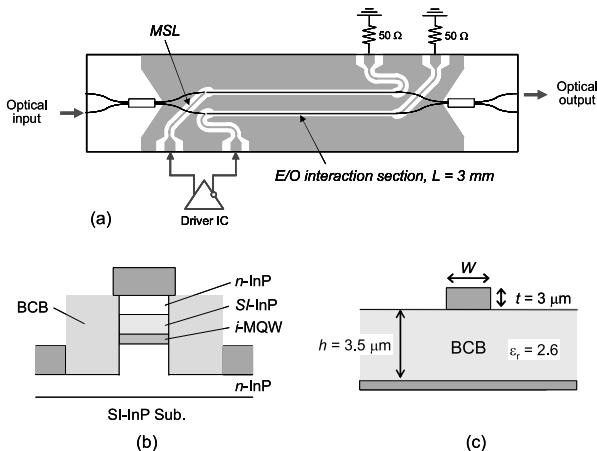
Fig. 1 Schematic diagrams of the dual-drive traveling-wave electrode Mach-Zehnder modulator. (a) Top view. (b) Cross-section of the *n-i-n* waveguide. (c) Cross-section of the microstrip line.

Fig. 2 Calculated characteristic impedance (a), and phase velocity (b) as a function of waveguide width.

Q) separate confinement heterostructure (SCH) layers. The *SI*-InP layer is $1.0\,\mu m$ thick. Owing to the deep Fe level, the *SI*-InP cladding layer acts as a potential barrier against the electron carriers from the upper *n*-doped cladding layer, and enables us to apply voltage efficiently across the core layer. There are two advantages to this structure. One is that no *p*-doped layer is introduced. This is beneficial in terms of optical loss. The other is attributed to the *n*-doped cladding layers on both sides of the signal and ground electrodes. Thanks to their high mobility and low contact resistance, the electrical loss remains small, and this results in a large modulation bandwidth. The low electrical and optical losses allow the modulator to operate at both a high bit rate and with a low driving voltage by lengthening the E/O interaction section.

The width of the waveguide and the thickness of the undoped layers, i.e. the MQW layer and the SCH layers, and the *SI*-InP cladding layer are important factors as regards controlling the waveguide capacitance so that the waveguide will satisfy the impedance matching and velocity matching requirements. Figure 2 shows the calculated characteristic impedance and the phase velocity as a function of optical waveguide width that we obtained using a commercially available high frequency structure simulator (HFSS). The dielectric constants used for the calculation are 12.4 for the semiconductor layers and 2.6 for the BCB. And the conductivity value used for the *n*-InP layer is 4.2×10^4 S/m. The conductivity value used for undoped core and *SI*-InP layers is 0 S/m since these layers have sufficiently high resistance. As shown in Fig. 2(a), the 50-Ω impedance matching requirement will be satisfied when the width is around $1.8\,\mu m$. And if we allow a margin of $\pm 5\,\Omega$, which corresponds to a −25-dB electrical reflection, the width tolerance is not severe, and ranges from 1.3 to $2.3\,\mu m$.

As regards the velocity matching condition, the electrical bandwidth f_0 is given by
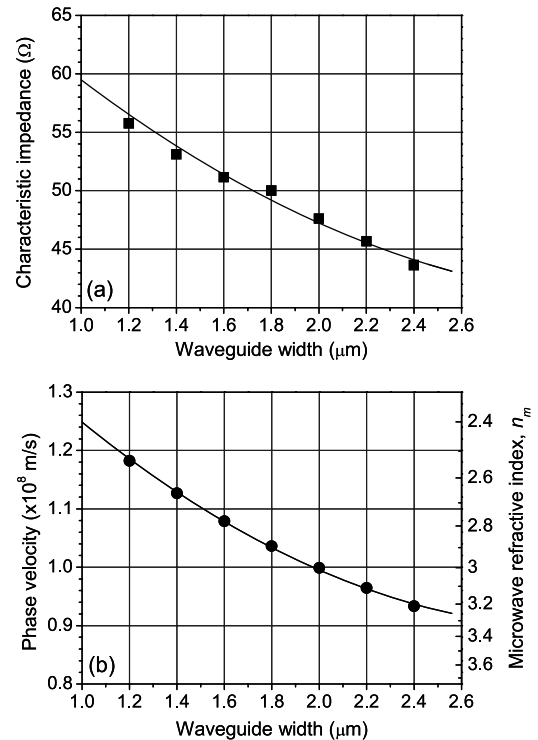
$$f_0 = 1.4c/(\pi|n_o - n_m|)L$$

where n_o and n_m are the optical and the microwave effective refractive indices, respectively, L is the length of the E/O interaction section, and c is the free-space velocity of light [10]. As a relatively strong electric field is produced in the core region of the *n-i-n* waveguide, an L of only several millimeters is required, and we set L at 3 mm for our device. So, the allowable absolute difference between the optical and electrical indices needed to achieve a 40-GHz bandwidth is about 1.1. The n_o of our waveguide is about 3.7, and so n_m should fall into the 2.6 to 4.8 range. The resulting n_m derived from Fig. 2(b) shows that this value is sufficiently large for our waveguide. From these calculated results and taking optical propagation loss and ease of fabrication into consideration, we chose $2.0\,\mu m$ for the optical waveguide width.

To facilitate connection with a differential output driver IC, the electrical input/output interface (GSG section) of the chip is placed on one side along the propagation axis. And we utilize microstrip lines (MSLs) from the GSG sections to the E/O interaction sections because they provide a small electrical loss, even when a bend has a small radius of curvature. This helps us to equalize the electrical length between the dual transmission lines in a small space. In other words, this contributes to keeping the chip small without requiring additional electrical phase adjustment. For our device, the radius is $50\,\mu m$. Figure 1(c) shows a schematic cross-section of the MSL and its parameters. And Fig. 3(a) shows the calculated characteristic impedance against the signal line width of the MSL. We found that a width of $8\,\mu m$ provides

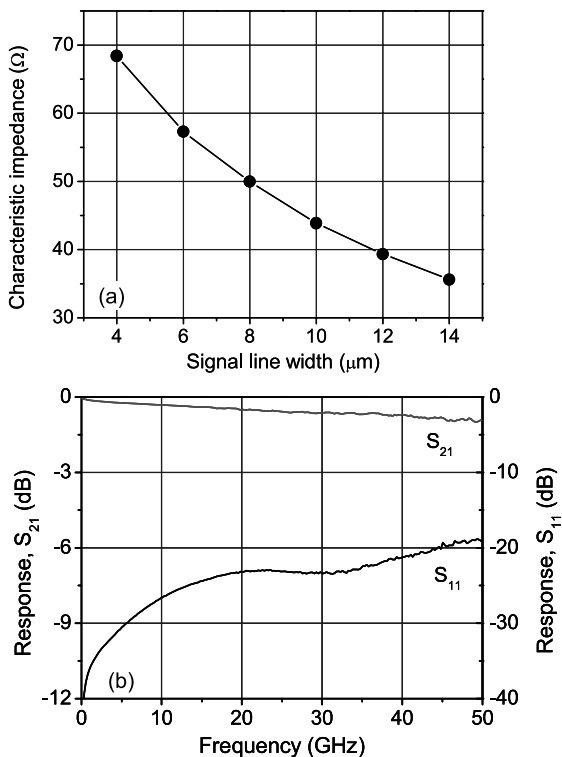**Fig. 4** Measured S-parameters of the fabricated chip.

Fig. 5 Photograph of the dual-drive Mach-Zehnder modulator module.

Fig. 3 Calculated characteristic impedance of the MSL as a function of signal line width (a), and measured S-parameters of the MSL part (b).

Fig. 6 Small signal optical response of the modulator module.

an impedance of $50\,\Omega$. And the impedance has a large tolerance as regards the signal line width. We measured the electrical transmission (S_{21}) and reflection (S_{11}) characteristics of the fabricated MSL part, which corresponds to a case where $L = 0\,mm$ (see Fig. 1(a)). We confirmed that there was very low electrical loss and reflection in the frequency range up to $50\,GHz$ as shown in Fig. 3(b). So, our structure can very easily provide both impedance and velocity matching and it also has a large fabrication tolerance. By introducing these techniques, we fabricated an InP-MZ modulator chip with a size of only $4.5 \times 0.8\,mm$.

3. Characteristics of MZ Modulator

First, we investigated the S-parameters of the fabricated chip itself by using GSGSG RF probes. As shown in Fig. 4 by the S_{21} curve, a 6-dB electrical-electrical (E/E) bandwidth of $46\,GHz$ was achieved. In addition, the reflection (S_{11}) was below $-18\,dB$, which is sufficiently small for practical use. Note that the two electrodes exhibit good uniformity in terms of frequency response. These results prove that our n-i-n structure is suitable for obtaining a high-modulation bandwidth and 50-Ω impedance matching.

Then, the fabricated InP-MZ modulator chip is installed in a compact package ($21\,mm$ (L) $\times$ $17\,mm$ (W) $\times$ $8\,mm$ (H)) whose footprint size is the same as those of conventional semiconductor laser modules [11]. Figure 5 shows a photograph of the modulator module. Two RF connectors for a differential electrical signal are placed on one side of
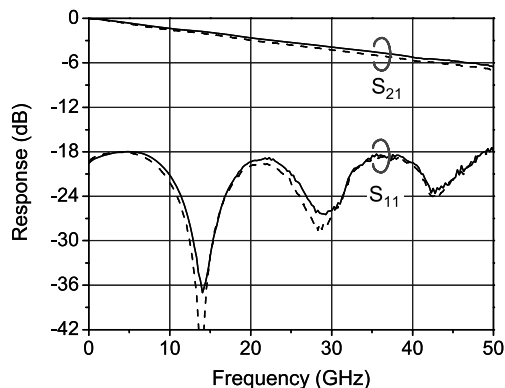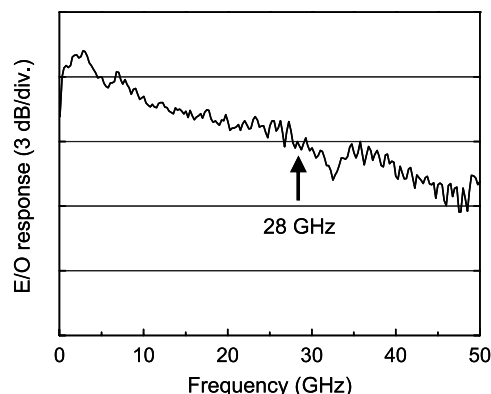
the package. The module contains 50-Ω terminations and bias tees.

The required switching voltage when the extinction ratio (ER) was more than $15\,dB$ was $2.2\,V$. The fiber-to-fiber insertion loss was $7\,dB$. As shown in Fig. 6, the measured small-signal 3-dB E/O bandwidth was $28\,GHz$, which is sufficiently large for the modulator to operate at $40\,Gb/s$.

We then investigated the dynamic performance. A 40-Gb/s NRZ signal with a PRBS of $2^{31} - 1$ was applied to each RF connector and the driving voltage for each port was only $1.3\,V_{pp}$. The operating wavelength was $1550\,nm$. Figure 7 shows the corresponding eye diagram and its bit-error-rate (BER) characteristics against the received average optical
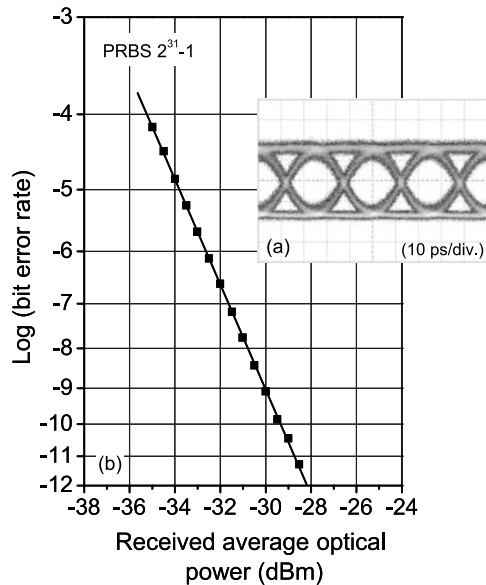
Fig. 7 40-Gb/s NRZ eye diagram in a push-pull configuration with a driving voltage of 1.3 V_{pp} (a), and the back-to-back bit error rate (b).

Fig. 8 10-Gb/s optical duobinary eye diagrams and bit-error-rate characteristics of the module. (a) Eye diagrams for back-to-back, 160-km, 200-km, and 240-km transmissions. (b) Bit error rates.

power. Clear eye opening was obtained. The dynamic extinction ratio (ER) was 10 dB. As shown in Fig. 7, we also confirmed error-free operation for a back-to-back configuration. These results indicate that our MZ modulator module has excellent characteristics, namely high-speed operation, a low driving voltage, and compactness.

We also investigated the 10-Gb/s optical DB transmission characteristics of the modulator [12], [13]. The optical DB format produces less spectral broadening than the conventional NRZ format and thus results in greater tolerance to chromatic dispersion and narrow-band optical filtering. These features are beneficial for optical reconfigurable add/drop multiplexing (ROADM) architecture with dense WDM (DWDM). As with many other advanced modulation formats, the optical DB signal can be generated by a dual-drive MZ modulator driven in a push-pull configuration with a differential electrical signal whose amplitude is the half-wavelength voltage (V_π). For such formats, the performance of the modulator including the resulting frequency chirp and the change in optical loss during modulation has a significant influence on the signal quality; therefore, this experiment is a good way to check the suitability of our modulator for advanced modulation formats.

The three-level electrical signal for the DB signal was obtained from a 10-Gb/s NRZ signal ($2^{31} - 1$ pseudorandom bit sequence) passed through a low-pass filter with a cut-off frequency of 2.8 GHz. The amplitude of the electrical signal was around 2.6 V_{pp}. The operating wavelength was set at 1550 nm, and the average launched optical power into the SMF was +3 dBm. Then, the optical DB transmission characteristics of signals traveling through 160, 200, and 240 km of SMF were investigated. The corresponding eye diagrams before and after transmission are shown in Fig. 8(a). We successfully obtained clear eye opening
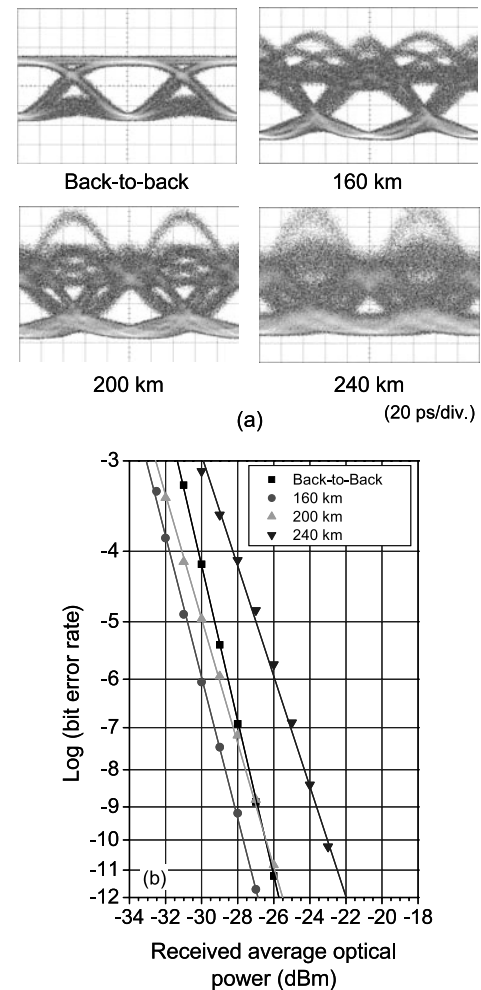
even after a 200-km transmission. The BER measurements revealed that error-free operation was achieved for all distances, and the power penalties were small, namely −1.0, 0.2, and 3.6 dB at BER = 10^{-12} for transmission distances of 160, 200, and 240 km, respectively. The 160-km transmission had a negative penalty because, with the DB signal, the cross point of the eye pattern for the back-to-back configuration is relatively high, and it becomes lower as the transmission distance increases. Accordingly, this makes the sensitivity after transmission over a certain distance better than that with a back-to-back configuration. These results agree with previous reports and confirm that our modulator and an LN-MZ modulator have comparable levels of performance [13]. Moreover, our modulator is superior in terms of power consumption because of its low driving voltage. In addition, the ample E/O bandwidth of our MZ modulator makes it possible to reduce the driving voltage further by lengthening the E/O interaction sections, or to generate optical DB signals with a higher bit rate. Thus, we can also say that our modulator is useful for advanced modulation formats.

4. Compact Wavelength Tunable Transmitter Module

A wavelength tunable transmitter module, in which a wavelength tunable laser is integrated with an MZ modulator, offers an attractive way to construct compact, cost-effective optical transponders/transceivers such as a 300-pin small form factor (SFF) transceiver. Some wavelength tunable transmitter modules have already been developed for both monolithic and hybrid integration [14], [15]. However, since the tunable lasers that they employ are all distributed Bragg reflector (DBR)-type lasers, they have the inherent problem of mode hopping. To avoid this, we employed a tunable laser array (TLA) based on the conventional distributed feedback (DFB) laser for our tunable transmitter module [16].

Figure 9 shows a photograph of the module. It consists of a TLA with a ten-DFB laser array, an *n-i-n* MZ modulator, and a wavelength locker [17]. The TLA and the MZ modulator are mounted on the same metal carrier and a thermo-electric cooler (TEC). They are coupled by using lenses via an isolator. The optical output from the MZ modulator is coupled into a fiber pigtail after passing through the wavelength locker, which is mounted on another TEC. All the lenses are welded by using a YAG laser to secure long-term stability and reliability. The module is 41 mm (L) × 13 mm (W) × 9 mm (H) in size, which is sufficiently small to realize a wavelength tunable transponder with a 300-pin SFF configuration.

Figure 10 shows the wavelength tuning characteristic of the module. The output wavelength can be tuned in a manner that selects an appropriate laser from the ten DFB lasers of the TLA, and then the temperature of the TLA chip is changed precisely over a range of 15 to 50 degrees as shown in Fig. 10(a). Our wavelength tunable transmitter covers wavelengths ranging from 1530 to 1562 nm. This
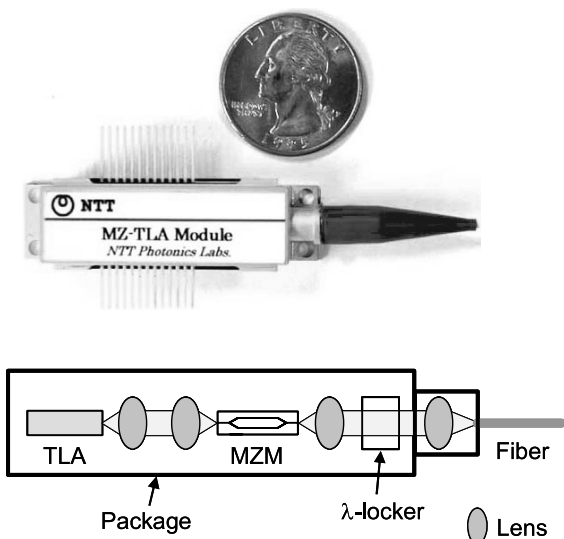
corresponds to 81 ITU-T channels with a 50 GHz spacing. For all channels, we obtained a CW module output power of more than 2 dBm (cf. Fig. 11) with a side mode suppression ratio of more than 50 dB.

The extinction curves for operating wavelengths of 1530, 1540, 1550, and 1560 nm are shown in Fig. 11 when a DC bias voltage was applied to one electrode of the modulator. Although both the operating wavelength and temperature were changed, the extinction curves reveal low sensitivity to these changes, and a V_π of around 2.5 V was obtained for all wavelengths (Fig. 11). And a negligible ex-
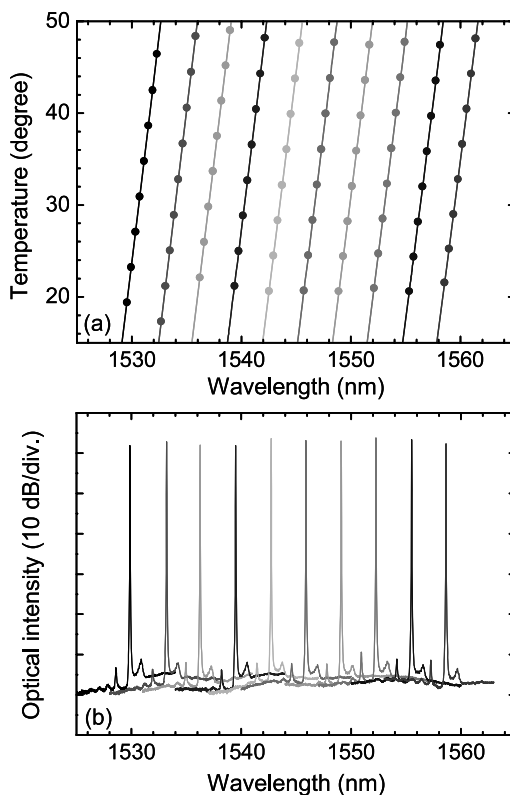

Fig. 10 Wavelength tuning characteristics and output spectrum of the module.
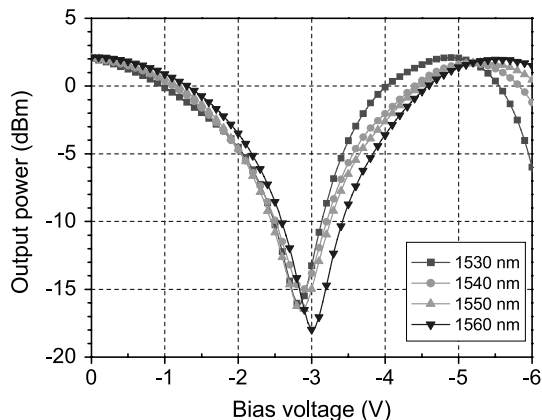

Fig. 9 Photograph and schematic drawing of the wavelength tunable transmitter module.

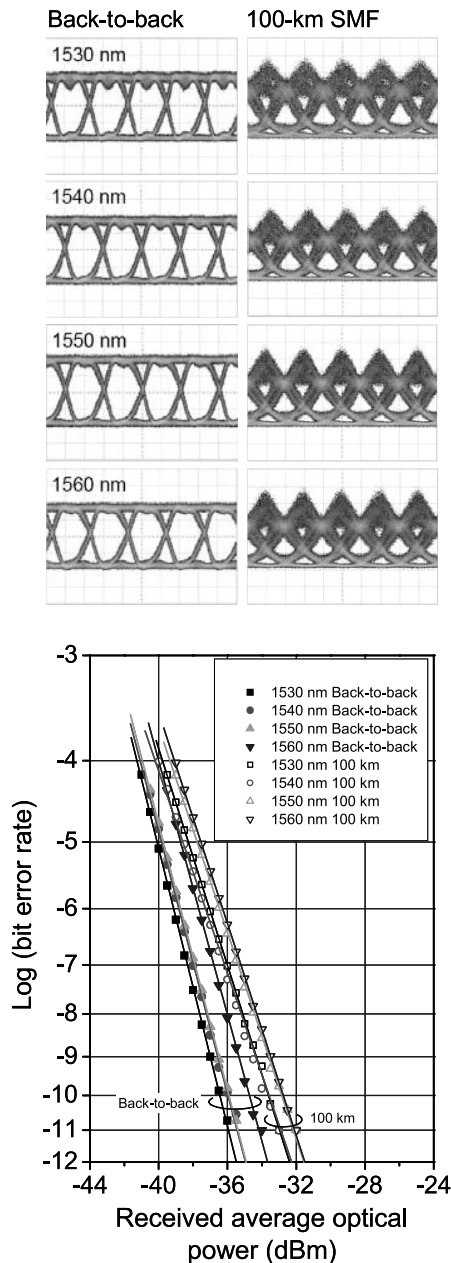**Fig. 11** Extinction characteristics of the module.

Fig. 12 BER performance at various wavelengths and eye diagrams for back-to-back and 100 km SMF transmissions.

cess loss was obtained even at $2 V_\pi$ (~ 5 V). This is because the absorption edge of the waveguide core is sufficiently detuned from the operating wavelength. In other words, the linear electro-optic effect (Pockels effect) dominates the modulation in our modulator, and so the wavelength dependence and absorption caused by quantum-confined stark effect (QCSE) can be reduced. The QCSE contribution to the modulation was estimated to be only one-fifth. Hence the *n-i-n* MZ modulator is very useful for our wavelength tunable transmitter.

Next, we demonstrate the dynamic performance of our transmitter module. The input electrical signal was a 10-Gb/s NRZ with a PRBS of $2^{31} - 1$ for the wavelengths de-

scribed above. In this experiment, we drove the MZ modulator in a push-pull configuration, and fixed the modulator driving condition even when the operating wavelength was changed. The bias voltages for the two electrodes were kept at -3.3 and -2.8 V, and the driving voltages applied to them were 0.75 and 2.25 V_{pp}. Under this driving condition, the modulated optical signal has a negative chirp, which is suitable for long-distance SMF transmission. With respect to the back-to-back configuration, we successfully obtained eye openings with a high dynamic ER of more than 10 dB for all wavelengths (cf. Fig. 12(a)). And we found that the eyes were clear even after a 100-km SMF transmission. Figure 12(b) shows the measured BERs for all wavelength channels. Error-free operation was confirmed. The sensitivity penalties resulting from the transmission were less than 3 dB. Therefore, our wavelength transmitter module makes it possible to realize highly reliable, compact, and inexpensive 10-Gb/s wavelength tunable transponders with a low power consumption.

5. Conclusion

We developed a compact dual-drive traveling-wave electrode InP-based MZ modulator. The modulator has a novel *n-i-n* waveguide structure that assists the modulator to operate at high speed and with a low driving voltage. The electrical input/output interface of the dual electrode is designed to be placed on one side of the chip to make it easy to connect with the differential driver ICs. We successfully used the fabricated modulator module in a push-pull configuration to generate a 40-Gb/s NRZ signal with a driving voltage of only 1.3 V_{pp}. Furthermore, we also generated a 10-Gb/s optical duobinary signal using the module, and transmitted it successfully over a 240-km SMF. This verifies the applicability of our modulator to advanced modulation formats. In addition, we demonstrated a compact wavelength tunable transmitter, in which the *n-i-n* MZ modulator was co-packaged with the TLA. 10-Gb/s NRZ operation over the entire C-band was confirmed. We believe that our modulator is a promising candidate for compact, cost-effective wavelength tunable transponders with low power consumption.

References

[1] C. Rolland, R.S. Moore, F. Shepherd, and G. Hillier, "10 Gbit/s 1.56 μm multiquantum well InP/InGaAsP Mach-Zehnder optical modulator," Electron. Lett., vol.29, no.5, pp.471–472, 1993.

[2] R. Spickermann, M.G. Peters, and N. Dagli, "A polarization independent GaAs-AlGaAs electrooptic modulator," J. Quantum Electron., vol.32, no.5, pp.764–769, 1996.

[3] M. Fetterman, C.P. Chao, and S.R. Forrest, "Fabrication and analysis of high-contrast InGaAsP-InP Mach-Zehnder modulators for use at 1.55-μm wavelength," IEEE Photonics Technol. Lett., vol.8, no.1, pp.69–71, 1996.

[4] L. Morl, C. Bornholdt, D. Hoffmann, K. Matzen, G.G. Mekonnen, and F.W. Reier, "A travelling wave electrode Mach-Zehnder 40 Gb/s demultiplexer based on strain compensated GaInAs/AlInAs tunnelling barrier MQW structure," IPRM98, WA3-4, 1998.

[5] K. Tsuzuki, T. Ishibashi, H. Yasaka, and Y. Tohmori, "Low driving voltage 40 Gbit/s n-i-n Mach-Zehnder modulator fabricated on

InP substrate," IEICE Trans. Electron., vol.E88-C, no.5, pp.960–966, May 2005.

[6] K. Yonenaga and S. Kuwano, "Dispersion-tolerant optical transmission system using duobinary transmitter and binary receiver," J. Lightwave Technol., vol.15, no.8, pp.1530–1537, 1997.

[7] R.A. Griffin and A.C. Carter, "Optical differential quadrature phase-shift keying (oDQPSK) for high capacity optical transmission," OFC2002, WX6, pp.367–368, 2002.

[8] A. Sano, H. Masuda, Y. Kisaka, S. Aisawa, E. Yoshida, Y. Miyamoto, M. Koga, K. Hagimoto, T. Yamada, T. Furuta, and H. Fukuyama, "14-Tb/s (140 × 111-Gb/s PDM/WDM) CSRZ-DQPSK transmission over 160 km using 7-THz bandwidth extended L-band EDFAs," ECOC2006, Th4.1.1, 2006.

[9] P.J. Winzer and R. Essiambre, "Advanced modulation formats for high-capacity optical transport networks," J. Lightwave Technol., vol.24, no.12, pp.4711–4728, 2006.

[10] R.G. Walker, "High-speed III-V semiconductor intensity modulator," IEEE J. Quantum Electron., vol.27, no.3, pp.654–667, 1991.

[11] K. Tsuzuki, H. Kikuchi, E. Yamada, H. Yasaka, and T. Ishibashi, "1.3-Vpp push-pull drive InP Mach-Zehnder modulator module for 40 Gbit/s operation," ECOC 2005, Th2.6.3, pp.905–906, 2005.

[12] T. Kurosaki, Y. Shibata, N. Kikuchi, K. Tsuzuki, W. Kobayashi, H. Yasaka, and K. Kato, "200-km 10-Gbit/s optical duobinary transmission using an n-i-n InP Mach-Zehnder modulator," IPRM2007, WeB1-3, 2007.

[13] A.J. Price, L. Pierre, R. Uhel, and V. Havard, "210 km repeaterless 10 Gb/s transmission experiment through nondispersion-shifted fiber using partial response scheme," IEEE Photonics Technol. Lett., vol.7, no.10, pp.1219–1221, 1995.

[14] J.S. Barton, M.L. Masanovic, A.T. Pedretti, E.J. Skogen, and L.A. Coldren, "Monolithically-integrated 40 Gbit/s widely-tunable transmitter using series push-pull Mach-Zehnder modulator SOA and sampled-grating DBR laser," OFC2005, OTuM3, 2005.

[15] R.A. Griffin, B. Pugh, J. Fraser, I.B. Betty, K. Anderson, G. Busico, C. Edge, and T. Simmons, "Compact, high power, MQW InP Mach-Zehnder transmitters with full-band tunability for 10 Gb/s DWDM," ECOC2005, Th2.6.2, pp.903–904, 2005.

[16] H. Oohashi, Y. Shibata, H. Ishii, Y. Kawaguchi, Y. Kondo, Y. Yoshikuni, and Y. Tohmori, "46.9-nm wavelength-selectable arrayed DFB lasers with integrated MMI coupler and SOA," IPRM2001, FBI-2, pp.575–578, 2001.

[17] K. Tsuzuki, N. Kikuchi, H. Sanjoh, Y. Shibata, K. Kasaya, H. Oohashi, H. Ishii, K. Kato, Y. Tohmori, and H. Yasaka, "Compact wavelength tunable laser module integrated with n-i-n structure Mach-Zehnder modulator," ECOC2006, Tu3.4.3, pp.79–80, 2006.

Ken Tsuzuki received B.S. and M.S. degrees in applied physics from Tohoku University in 1993 and 1995, and was awarded a Ph.D. in 2006. In 1995 he joined NTT Opto-electronics Laboratories. Since then, he has been engaged in the research and development of semiconductor photonic devices for optical fiber communication systems. From 2001 to 2002 he was with NTT Electronics Corporation. Now he is a Research Engineer at NTT Photonics Laboratories and is engaged in the research and development of semiconductor photonic devices. Dr. Tsuzuki is a member of the Japan Society of Applied Physics.

Takeshi Kurosaki received the B.S. degree and M.S. degree in electronics engineering from Hokkaido University, Sapporo, Japan, in 1987 and 1989, respectively. In 1989, he joined the Opto-electronics Laboratories, Nippon Telegraph and Telephone Corporation (NTT), Atsugi. Since then, he has been engaged in research on high-performance distributed-feedback (DFB) lasers and low-cost optical modules for optical transmission systems. Mr. Kurosaki is a member of the Japan Society of Applied Physics.

Yasuo Shibata received B.E. and M.E. degrees in electrical engineering from Keio University, Kanagawa, Japan in 1985 and 1987, respectively. In 1987, he joined NTT Optoelectronics Laboratories, Nippon Telegraph and Telephone Corporation (NTT), Kanagawa, Japan, where he has been engaged in research on optical switches, optical filters and integrated devices. He is currently with NTT Photonics Laboratories, and is engaged in research on SOAs, SOA-based functional devices and modulators. He is a Senior Research Engineer in the Photonic Device Laboratory of NTT Photonics Laboratories. Mr. Shibata is a member of the Japan Society of Applied Physics.
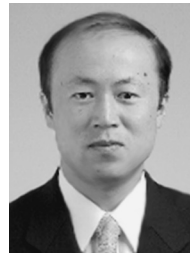
Nobuhiro Kikuchi received B.E. and M.E. degrees in electrical and electronics engineering from Kobe University, Hyogo, Japan, in 1995 and 1998, respectively. In 1998 he joined NTT Opt-electronics Laboratories, and since 1999, he has been with NTT Photonics Laboratories and is engaged in research on optical semiconductor devices and their integrated devices for optical communication networks. He is currently a Research Engineer at NTT Photonics Laboratories. Mr. Kikuchi is a member of the Japan Society of Applied Physics.

Hiroshi Yasaka received B.S. and M.S. degrees in physics from Kyushu University in 1983 and 1985, and was awarded a Ph.D. in Electronics Engineering from Hokkaido University in 1993. In 1985 he joined Atsugi Electrical Communication Laboratories, Nippon Telegraph and Telephone Corporation (NTT). Until 2008, he was engaged in the research and development of semiconductor photonic devices for optical fiber communication systems. In 2008 he joined the Research Institute of Electrical Communication (RIEC) at Tohoku University as a professor and has been engaging in research on highly functional semiconductor photonic devices and their monolithically integrated devices. Professor Yasaka is a member of the Japan Society of Applied Physics (JSAP).